A broad spectrum of actin paralogs in *Paramecium tetraurelia* cells display differential localization and function

Ivonne M. Sehring*, Christoph Reiner, Jörg Mansfeld, Helmut Plattner and Roland Kissmehl

Department of Biology, University of Konstanz, P.O. Box 5560, 78457 Konstanz, Germany

*Author for correspondence (e-mail: ivonne.sehring@uni-konstanz.de)

Accepted 23 October 2006
Journal of Cell Science 120, 177-190 Published by The Company of Biologists 2007
doi:10.1242/jcs.03313

Summary

To localize the different actin paralogs found in *Paramecium* and to disclose functional implications, we used overexpression of GFP-fusion proteins and antibody labeling, as well as gene silencing. Several isoforms are associated with food vacuoles of different stages. GFP-actin either forms a tail at the lee side of the organelle, or it is vesicle bound in a homogenous or in a speckled arrangement, thus reflecting an actin-based mosaic of the phagosome surface appropriate for association and/or dissociation of other vesicles upon travel through the cell. Several paralogs occur in cilia. A set of actins is found in the cell cortex where actin outlines the regular surface pattern. Labeling of defined structures of the oral cavity is due to other types of actin, whereas yet more types are distributed in a pattern suggesting association with the numerous Golgi fields. A substantial fraction of actins is associated with cytoskeletal elements that are known to be composed of other proteins. Silencing of the respective actin genes or gene subfamilies entails inhibitory effects on organelles compatible with localization studies. Knock down of the actin found in the cleavage furrow abolishes cell division, whereas silencing of other actin genes alters vitality, cell shape and swimming behavior.

Supplementary material available online at
http://jcs.biologists.org/cgi/content/full/120/1/177/DC1

Key words: Actin, Cytoskeleton, Microfilaments, *Paramecium*, Trafficking

Introduction

Actin, an abundant cytoskeletal protein, is of paramount importance in forming the cell cortex, amoeboid movement, cyclosis, vesicle trafficking, cell division and for cell contraction etc. In the past few years, new aspects have emerged. This includes a contribution to docking of dense-core secretory vesicles (Gasman et al., 2004), endocytosis (Merrifield et al., 2002; Merrifield, 2004; Kirkham and Parton, 2005; Yarar et al., 2005; Kaksonen et al., 2006), arrangement of Golgi elements (Lin et al., 2005), formation of Golgi-derived vesicles (Carreno et al., 2004; Cao et al., 2005) and numerous interactions with phagocytic as well as endocytic and lysosomal vesicles of different stages (Damiani and Colombo, 2003; Drengk et al., 2003; Stoorvogel et al., 2004; Yam and Theriot, 2004; Kjeken et al., 2004; Hölttä-Vuori et al., 2005). A universal function of F-actin is the formation of the cleavage furrow in animal cells (Otegui et al., 2005). A plethora of proteins interacting with actin further contribute to the dynamics and specificity of actin interactions (Pollard et al., 2000). Such interactions allow for a broad diversification of the actin cytoskeleton, even though some lower eukaryotes possess only one actin gene (García-Salcedo et al., 2004), whereas humans have six (Pollard, 2001). The closely related ciliate *Tetrahymena thermophila* possesses four actin genes (Williams et al., 2006). In addition, a range of actin-like proteins (ALP) and actin-related proteins (ARP) exist (Goodson and Hawse, 2002; Kandasamy et al., 2004; Muller et al., 2005). Apicomplexan parasites (*Plasmodium*, *Toxoplasma*), close relatives of our non-parasitic ciliates, mostly contain a single conventional actin and several ARPs, of which some are unique to apicomplexans (Gordon and Sibley, 2005).

The ciliated protozoan *Paramecium* is a highly organized unicellular organism with an elaborate ultrastructure (Fig. 1). We now can show a widely diversified set of genes encoding actin and ARP in *Paramecium* (Table 1) (I.M.S., J.M., C.R., E. Wagner, H.P. and R.K., unpublished). Indirectly the question as to why this multiplicity has evolved, probably by gene duplications (Ruiz et al., 1998; Aury et al., 2006), and maintained during evolution, is addressed in this paper in the context of localization and functional analyses. These reveal differential positioning and functional engagement, in established vesicle trafficking pathways and beyond. Microfilaments of actin might play a role in transport to the cell cortex and the recognition of the docking sites by trichocysts (Beisson and Rossignol, 1975).

We used overexpression as green fluorescent protein (GFP) fusion proteins, eventually complemented by antibody localization and silencing of the respective genes by RNAi. Because of the abundance of many isoforms (Table 1), not all could be analyzed in detail.

In most species, actin is sensitive to drugs that stabilize either G-actin (cytochalasin B or D, latrunculin A) or F-actin (phalloidin, jasplakinolide) (Wieland and Faulstich, 1978;

Table 1. Actin and actin-related proteins in *P. tetraurelia*

Gene	Subfamily	Accession number	Protein Identity* (%)	Protein Identity*,† (%)
*actin*1	*act1-1*	AJ537442	100	100
	act1-2	AJ537443	100	100
	act1-3	AJ537444	100	100
	act1-4	AJ537445	89.9	89.9
	act1-5	CR855974	91.5	91.5
	act1-6	CR548612	61.7	61.7
	act1-7	CR855973	76.9	76.9
	act1-8	CR855972	70.2	70.2
	act1-9	CR855988	63.3	63.3
	act1-10‡	CR855989	10.9	12.2
*actin*2	*act2-1*	AJ537446	100	59.6
	act 2-2	AJ537447	99.5	59.6
*actin*3	*act 3-1*	AJ537448	100	44.1
	act 3-2	CR548612	82.7	44.7
*actin*4	*act 4-1*	CR855971	100	28.2
	act 4-2	CR856039	96.8	28.5
*actin*5 (*ARP*1)§	*act 5-1*	CR855970	100	39.6
	act 5-2	CR855969	100	39.6
	act 5-3	CR855968	86.7	39.1
*actin*6	*act 6-1*	CR855967	100	30.9
	act 6-2	CR855986	93.7	31.1
*actin*7 (*ARP*4)§	*act 7-1*	CR855941	100	23.7
	act 7-2	CR855965	95.4	25.0
*actin*8	*act 8-1*	CR548612	100	37.0
*actin*9 (*ARP*10)§	*act 9-1*	CR855964	100	17.6

*Comparison of family members. Sequences were aligned using the Clustal W method.
†All identities refer to act1-1.
‡Putative pseudogene.
§In the NCBI database, these paralogs are in part assigned to ARP or actin.

Visegrády et al., 2004). However, in lower eukaryotes the situation is rather complex. For instance, Apicomplexan parasites (*Plasmodium*, *Toxoplasma*), close relatives of our non-parasitic ciliates, contain abundant actin, mainly in monomeric or short polymeric forms (Dobrowolski et al., 1997; Poupel et al., 2000; Schmitz et al., 2005; Sahoo et al., 2006). Also surprising is the inability of any previous work to visualize in *Paramecium* a cleavage furrow by fluorescent phalloidin (Kersken et al., 1986a) whereas phagocytosis could easily be inhibited by cytochalasins (Cohen et al., 1984; Allen and Fok, 1985; Fok et al., 1985; Allen et al., 1995).

We now show that the specific localization of different actin isoforms in *Paramecium* is paralleled by functional diversification. Analysis of *Paramecium* cells appears to be rewarding as they display a most elaborate membrane-trafficking system (Fig. 1), with distinct, predictable pathways (Allen and Fok, 1983; Allen and Fok, 2000; Fok and Allen, 1988; Fok and Allen, 1990; Plattner and Kissmehl, 2003) in which the different actin isoforms participate, as we now show. In the present work we combined the different techniques to establish a functional and topological overview of actin diversification in a *Paramecium* cell.

Results

Actin isoforms and their localization

Based on a *Paramecium* genome data base search (I.M.S., J.M., C.R., E. Wagner, H.P. and R.K., unpublished), Table 1 summarizes the actin isoforms considered in the present work. Essentially we found nine subfamilies of actin genes (ten members of subfamily 1, two or three members in the other subfamilies) and two subfamilies of ARP (with one or two members each), with identities on the amino acid level ranging between 100% and 63% (for members of the actin1 subfamily) and 60% to 18% for the other subfamilies, when referred to *Paramecium* actin1 (Table 1). In comparison with actins in other organisms, actins in *P. tetraurelia* are highly divergent, which makes an accurate classification difficult. Owing to contradictory hits within blast searches in the NCBI database and alignments with ARPAnno [an actin-related protein annotation server designed by Muller et al. (Muller et al., 2005)], some *P. tetraurelia* subfamilies could be assigned to both actins and ARPs. For example, NCBI Blast searches with actin9 leads to hits for both actins and ARP10 of other organisms, whereas ARPAnno alignment resulted in an equally low score for ARP2 and orphans (sequences lacking common defining characteristics), with the score being below the value which was determined as reliable by the designers. As other sequences could be clearly assigned to ARP2 (data not shown), we rely on the NCBI Blast search results for the classification of our sequences. To investigate the subcellular localization of the different actin isoforms, GFP constructs were made. For the isoforms act1-2, act1-6, act1-9, act2-1, act3-1, act5-1, act6-1 and act8-1, the open reading frame was cloned into pPXV-eGFP (Hauser et al., 2000), the *Paramecium* overexpression vector (Haynes et al., 1995). Previously, a GFP-actin construct was used to transform *T. thermophila* cells, which led to a failure of nuclear elongation and cytokinesis (Hosein et al., 2003). In contrast to the construct used in that work, we fused the GFP gene to the 5′ end of the actin gene with an 11 amino acid spacer interspersed to avoid any possible disturbance of folding and polymerization because of the GFP tag (Doyle and Botstein, 1996; Wetzel et al., 2003). None of our constructs led to any cell abnormalities. The plasmids (~5 μg/μl) were introduced into postautogamous *Paramecium* cells by microinjection into the macronucleus and GFP fluorescence was analyzed in descendants of the injected cells. A summary of the subcellular localization of the actin isoforms investigated is given in Table 2.

Actin subfamily 1

To take into account the wide diversification of the actin1 subfamily (Table 1), the subcellular localization of the isoforms act1-2, act1-4, act1-6 and act1-9 were examined in more detail. GFP-act1-2 formed comet tails at food vacuoles, which propelled them through the cytoplasm (Fig. 2A-C). Alternatively it might be accumulated in patches at the surface of food vacuoles (Fig. 2D-F). Transformation with GFP-act1-4 resulted in diffuse fluorescence throughout the cytoplasm (data not shown), as with GFP-act1-6 (Fig. 2G,H). With GFP-act1-9, pronounced comet tails could be observed, which propelled food vacuoles even in opposite directions through the cytoplasm, with the tail always at the rear side (Fig. 2I-N and supplementary material, Movie 1). These GFP-act1-9 comet tails could not be observed on every food vacuole because they were very dynamic structures, which have rapidly polymerized and depolymerized. Furthermore, thin, very dynamic tails were also seen to propel smaller vesicles. At the posterior end of the oral cavity, GFP-act1-9 filaments could be observed which were catapulted into the cytoplasm (see supplementary material Movie 1).

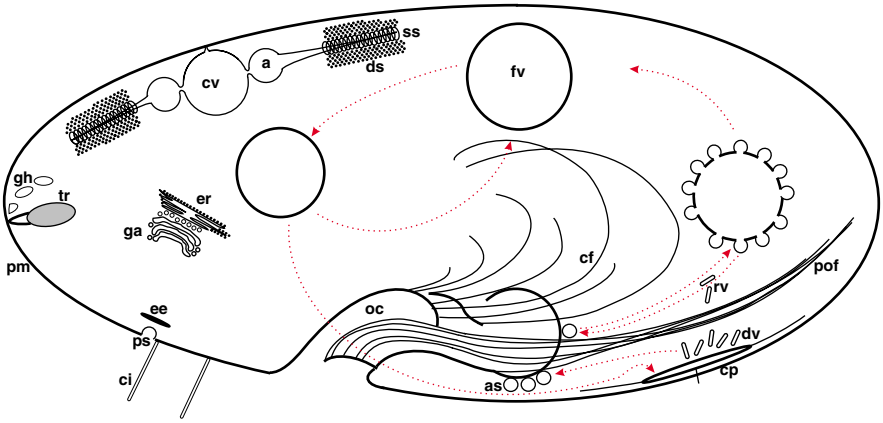

Fig. 1. Schematic *Paramecium* cell. The plasma membrane (pm) is covered with cilia (ci). Along the oral groove, they beat rhythmically to wash food towards the oral cavity (oc). The phagosomal apparatus consists of several elements: as, acidosomes mediating acidification of a food vacuole (fv) after pinching off; cytopharyngal fibers (cf), post oral fibers (pof), cytoproct (cp, site of exocytotic release of spent phagosomes). Dense-core vesicles (trichocysts, tr), are attached to the plasma membrane. Osmoregulation is executed by two contractile vacuole complexes (a, ampula; cv, contractile vacuole; ds, decorated spongiome; ss, smooth spongiome). The red arrows indicate transport routes during phagosomal processing. Discoidal vesicles (dv) and other recycling vesicles (rv) are responsible for return transport of membranes. The endosomal system, composed of parasomal sacs (ps) and early endosomes (ee), is arrayed in a regular fashion. er, endoplasmatic reticulum; ga, golgi apparatus.

Actin3-1

Transformation of *Paramecium* cells with GFP-act3-1 resulted in a diffuse staining of the cytoplasm, although a specific labeling also could be observed (data not shown). A GFP signal was found at the surface of food vacuoles, but in this case the vacuoles were almost completely surrounded by a layer of GFP-act3-1 of variable thickness. To enhance the GFP fluorescence, anti-GFP antibodies were applied to transformed cells. In the cell cortex, GFP-act3-1 outlined the ridges of the egg-carton-like cell surface relief typical of *Paramecium* cells, as well as cilia (Fig. 3).

Actin4-1

Localization of GFP-act4 was not possible because cells did not divide after microinjection and were too sensitive for observation under the microscope. Therefore, we raised a polyclonal antibody against a 160-residue peptide of act4-1 to obtain subfamily-specific antibodies. The region chosen has less than 25% identity to other subfamilies, which makes it unlikely that the antibodies will react with any of the other actins or ARPs. The antibodies were affinity purified not only against the peptide for immunization, but also against peptides used to raise antibodies against act1-1 (Kissmehl et al., 2004) and against act5-1, and were tested in western blots for their crossreactivity, which was negative (Fig. 4A). Immunolocalization studies with anti-act4antibodies showed labeling of the oral cavity, around nascent food vacuoles (Fig. 4B), in cilia and in the cell cortex (Fig. 4C). In dividing cells, a weak labeling of the micronucleus separation spindles could be observed (data not shown). The most striking labeling was that of the cleavage furrow, with which act4 was associated from the beginning of an early stage of division until fission was completed (Fig. 4D,F). For comparison, act5-1-specific antibodies did not label the cleavage furrow (Fig. 4G).

Table 2. Localization of the different actin isoforms

	GFP localization									AB localization		
	actin1-2	actin1-4	actin1-6	actin1-9	actin2-1	actin3-1	actin5-1	actin6-1	actin8-1	actin1-1*	actin4-1	actin5-1
Cortex	–	–	–	–	–	+	+	–	+	+	+	+
Oral cavity	–	–	–	–	–	–	+	–	+	+	+	+
Oral filaments	–	–	–	–	–	–	+	–	+	–	–	+
Phagosomes	+	–	–	+	–	+	+	–	+	+	–	+
Cilia	–	–	–	–	+	+	–	–	–	+	+	+
Cytosolic compartment	–	+	+	–	+	+	–	+	–	–	–	–
Cleavage furrow	–	–	–	–	–	–	–	–	–	–	+	–

For the isoforms act1-2, act1-6, act1-9, act2-1, act3-1, act5-1, act6-1 and act8-1, GFP constructs were used to transform cells and to analyze different localization of the GFP-fusion proteins in descendants. Cells transformed with a GFP-act4-1 construct did not divide and were too instable for localization studies. Therefore, specific antibodies were raised against act4-1. In addition, antibodies against act5-1 were raised. Anti-act5-1 antibodies labeled the same structures as seen with GFP-act5-1 except for the labeling of the cilia. The GFP-signal might not be detected because of the fast movement of cilia, in contrast to immunodetection. *As the actin isoforms act1-1, act1-2 and act1-3 are identical at the amino acid level (I.M.S., J.M., C.R., E. Wagner, H.P. and R.K., unpublished), the polyclonal antibodies against act1-1 will also recognize those isoforms and probably also peptides from further members of the act1 subfamily and possibly also of other subfamilies (Kissmehl et al., 2004).

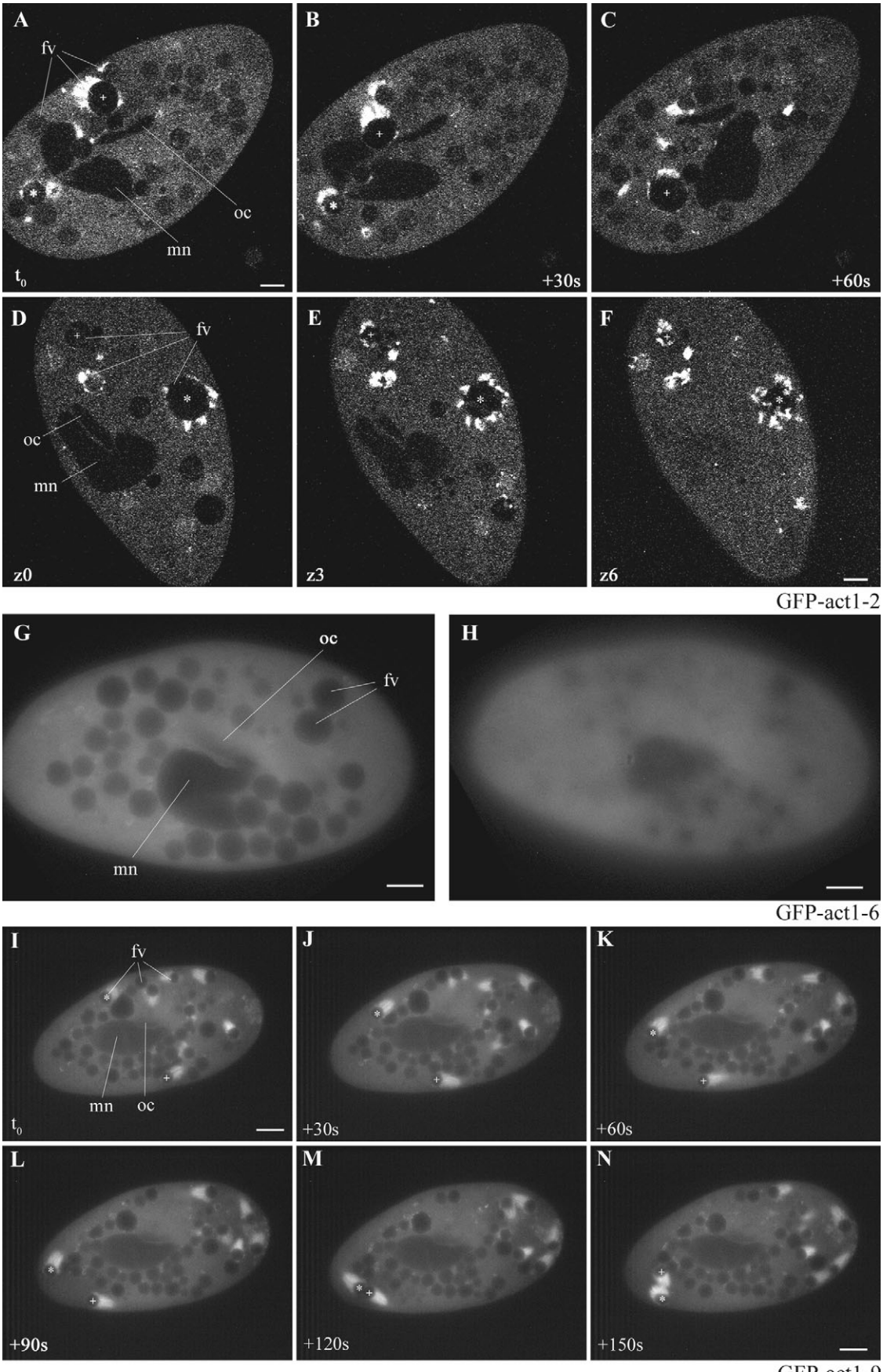

Fig. 2. See next page for legend.

Fig. 2. GFP localization of members of the act1 subfamily. (A-C) A confocal time series of a cell transformed with GFP-act1-2 reveals actin comet tails that propel vacuoles (two labeled * and +) through the cytoplasm. (D-F) Confocal z series of a cell transformed with GFP-act1-2. Note the irregular distribution of patches around the surface of some food vacuoles (fv). (G,H) Transformation with GFP-act1-6 resulted in diffuse cytosolic staining without any specific localization (G, median; H, superficial plane). (I-N) In cells transformed with GFP-act1-9, actin comet tails on food vacuoles occurred. Food vacuoles can move in opposite directions through the cytoplasm (see the movement of the two vacuoles labeled with * and + within 150 seconds). See supplementary material Movie 1 for the thin, very dynamic tails that can propel some food vacuoles and small vesicles through the cytoplasm and actin filaments that are catapulted into the cytoplasm from the posterior end of the oral cavity. mn, macronucleus; oc, oral cavity; fv, food vacuoles. Bars, 10 μm.

Actin5-1

Transformation of *Paramecium* cells with GFP-act5-1 resulted in a discrete labeling around a sub-set of food vacuoles. In contrast to the labeling observed with other GFP constructs at food vacuoles, GFP-act5-1 formed neither patches nor tails but a fine ring on the surface of the respective food vacuoles. Indeed, there was no consistent covering of the whole food vacuole (arrowhead in Fig. 5A), and the label could not be found around all food vacuoles (Fig. 5A,B). At the oral cavity, the following structures were labeled: (1) Two half-moon-shaped labeled structures assigned to the peniculus (Fig. 5B); (2) a dynamic fiber system emanating into the cytoplasm (arrow in Fig. 5B) anchored by a wreath-like structure with pointed pattern, probably the quadrulus of the oral cavity. (Note that the cell shown in Fig. 5A contains numerous autofluorescent crystals.) Immunolocalization studies with affinity-purified antibodies against act5-1 showed similar localization to that observed with GFP-tagged act5-1 (Fig. 4G), thus excluding possible artifacts resulting from GFP overexpression or fixation/permeabilization during preparation for immunolocalization studies.

Actin8-1

The fluorescent signals obtained with GFP-act8-1 were in many cases similar to those obtained with GFP-act5-1. Labeling around single food vacuoles could be observed, but in contrast to the incomplete envelopment with GFP-act5-1, the food vacuoles seem to be entirely covered (Fig. 6A,C). The two half-moon-shaped structures at the presumed peniculus and the curved structure of the presumed quadrulus are also labeled, and a dynamic fiber system that originates from the latter could be observed (Fig. 6A-C, supplementary material Movie 2 and Fig. S1). Careful comparison of cells transformed with GFP-act5-1 with cells transformed with GFP-act8-1 showed that one probably deals with two different fiber systems emanating from the oral cavity. Beyond that, focusing on the surface of transformed cells revealed regular rows of small dots underneath the plasma membrane, arranged ~2 μm apart (Fig. 6D), which can easily be identified as 'parasomal sacs'. They correspond to stationary sites of constitutive exocytosis and coated pit endocytosis (Allen and Fok, 2000; Plattner and Kissmehl, 2003).

Furthermore, small point-like to rod-shaped organelles could be observed (arrow in Fig. 6B) which, particularly in z-stacks (data not shown), showed some enrichment towards the cell surface. These organelles were smaller than 1.0 μm and did not move with the cyclosis stream. In electron microscope immunoanalysis with cells overexpressing GFP-act8, using anti-GFP antibodies followed by protein A coupled to 5 nm gold particles (pA-Au_{5nm}), we frequently found labeling at the periphery of the rough endoplasmic reticulum (ER) in association with smooth vesicular membrane-bounded elements (Fig. 6E,F). These may represent Golgi elements with some deformation, possibly as a result of the overexpression of actin (García-Salcedo et al., 2004). The fixation used preserves F-actin, its position in filaments and its antigenicity as shown in the literature.

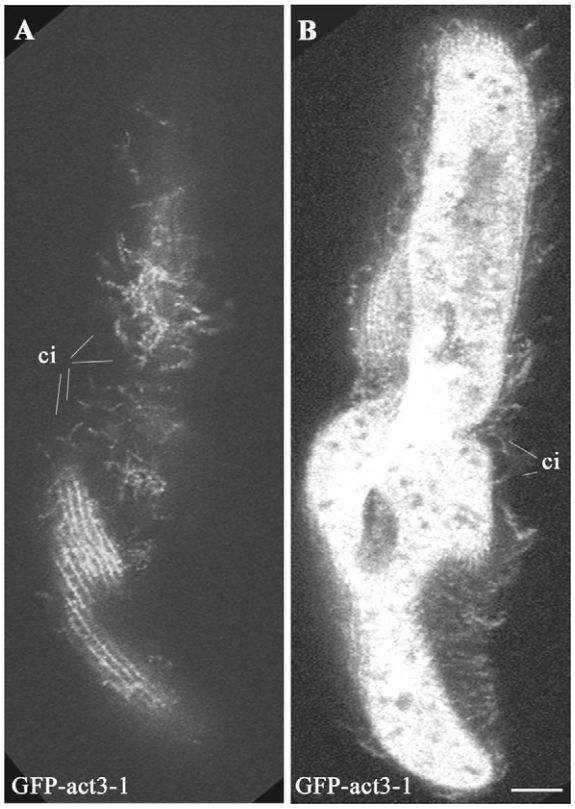

Fig. 3. Application of an anti-GFP antibody to cells transformed with GFP-act3-1 constructs. Confocal images from superficial (A) and median (B) focal planes of a dividing cell. Note labeling of cilia (ci), labeling of the cortical 'egg-box' relief in A and diffuse staining of the cytoplasm in B. The cleavage furrow is not labeled. Bars, 10 μm.

Actin2-1 and actin6-1

GFP localization of act2-1 and act6-1 resulted in a diffuse staining all over the cytoplasm, with no specific highlighted structure. This is similar to the results obtained with GFP-act1-6. However, enhanced with anti-GFP antibodies, GFP-act2-1 is found in cilia (data not shown). The different subcellular localizations achieved by a GFP tag of specific isoforms or subfamily-specific antibodies are summarized in Table 2 and, with the inclusion of previous data, in the final schematic Fig. 11.

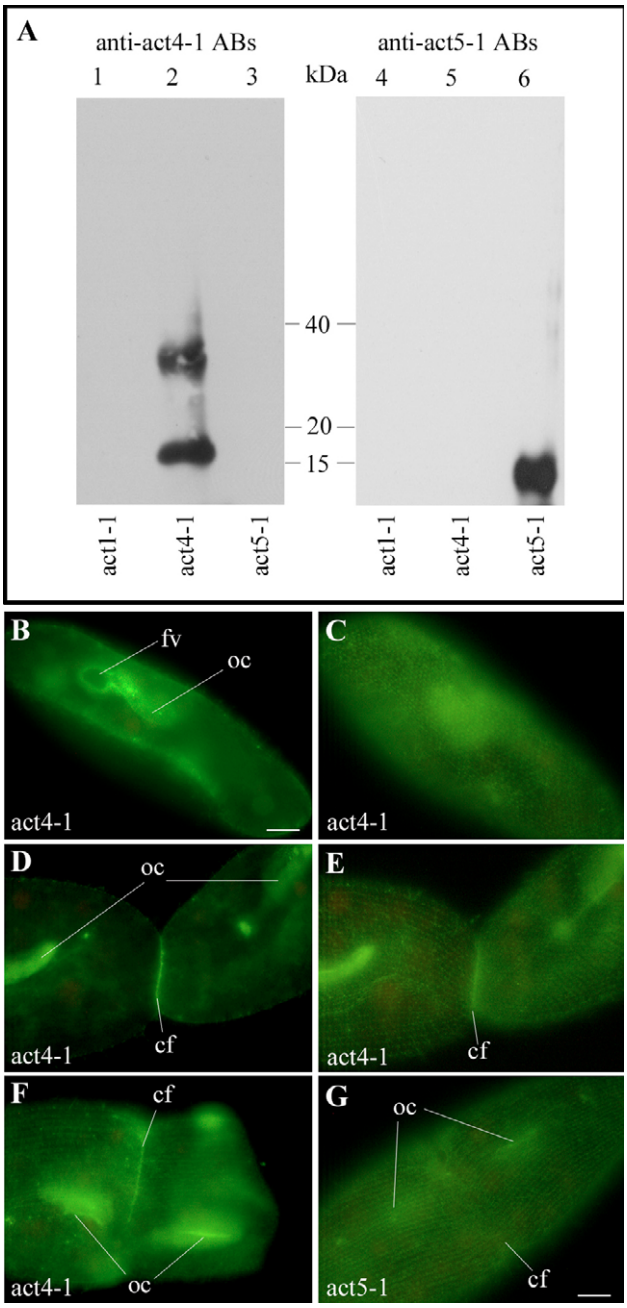

Fig. 4. Immunolocalization of actin using subfamily-specific antibodies. (A) Western blot analysis of affinity-purified anti-act4-1 antibody (lanes 1-3) and anti-act5-1 antibody (lanes 4-6) against the recombinant act1-1 (L_{261}-G_{366}; lanes 1, 4), act4-1 (M_1-A_{160}; lanes 2, 5) and act5-1 peptides (H_{175}-L_{290}; lanes 3, 6), respectively. There is no crossreactivity between the isoforms. The double band in lane 2 is probably due to formation of dimers. (B-E) Localization of act4. (B,C) Median and superficial focus plane showing labeling of the oral cavity (oc), around a nascent food vacuole (fv), of cilia and at the cell cortex. (D,E) Median and superficial plane of a dividing cell. Note labeling of the cleavage furrow (cf) and of the old and new oral cavity (oc). (F) Superficial plane of a cell in an earlier stage of division. Again the cleavage furrow is labeled, as well as the old and the new oral cavities. (G) For comparison, a cell in the same dividing state as F, but labeled with an anti-act5 antibody, reveals no labeling of the cleavage furrow. Bars, 10 μm.

RNA interference by feeding

For functional analysis of the different actin subfamilies, gene-silencing experiments were performed using the RNAi approach by feeding. *Paramecium* cells were fed with *E. coli* expressing double-stranded RNA coding for a specific actin, which elicits a small interfering RNA-mediated silencing process of the target genes. As a negative control, the empty feeding vector (pPD) was used for mock silencing. To ascertain the reliability of the RNAi-based feeding procedure, we performed controls with the pPD-nd7 construct (Skouri and Cohen, 1997). Silencing of the nd7 ('nondischarge') gene successfully suppressed exocytosis of trichocysts. The effects of gene silencing on various behavioral and physiological aspects were examined. In detail, cell shape, cyclosis, exocytotic capacity, the contraction period of the contractile vacuoles, phagocytotic capacity, the general swimming behavior and the swimming reaction upon depolarization and hyperpolarization were analyzed. For each actin subfamily, one gene was cloned into the silencing vector. Within the respective subfamilies, the nucleotide identity is high enough to expect co-silencing (Ruiz et al., 1998). An exception is the large actin1 subfamily with ten members that vary up to 35%. Therefore, constructs for the specific isoforms act1-2, act1-6 and act1-9 were made. With none of these constructs could we observe any behavioral or functional effect (Table 3). Potentially, several genes of subfamily 1 are functionally redundant, as we could observe similar localization patterns (GFP-act1-2 similar to GFP-act1-9, and GFP-act1-6 to GFP-act1-4).

To confirm co-silencing within the subfamilies, and to exclude any functional compensation by the unsilenced paired isoform, we tested a construct where both isoforms of the actin3 subfamily, act3-1 and act3-2, were cloned in tandem. RNAi with this construct gave identical results compared with those obtained with the isoform act3-1 alone (Table 3). To exclude silencing variation resulting from the length of the introduced dsRNA or cross-silencing of other subfamilies, constructs of different lengths were designed for act2-1 and act3-1. Within both subfamilies, all constructs showed the same effects. A summary of the results obtained with the different gene silencing constructs is given in Table 3.

Cell division

The number of cell fissions per day was calculated to see if silencing of any of the actin subfamilies affects the growth rate of *Paramecium*. In general, a slightly reduced division rate could be observed 24 hours after the start of the feeding experiment, probably because of slower division of cells recovering from autogamy and the change of the bacteria used for feeding. Cell growth was not influenced by most of the silencing constructs (Fig. 7). Only silencing of act4 or act9 resulted in a significant reduction of the division rate. Silencing of act9 led to half of the division rate, whereas cells silenced in act4 could not divide anymore and subsequently died.

Cell shape

We could recognize changes in the general cell shape after silencing of act4, act7 or act9. Act4-silenced cells were arrested during division and, according to their shape, named 'boomerang' (Fig. 8A). Cells silenced in act7 were generally enlarged with a pointed anterior end, called 'dolphin' (Fig. 8B).

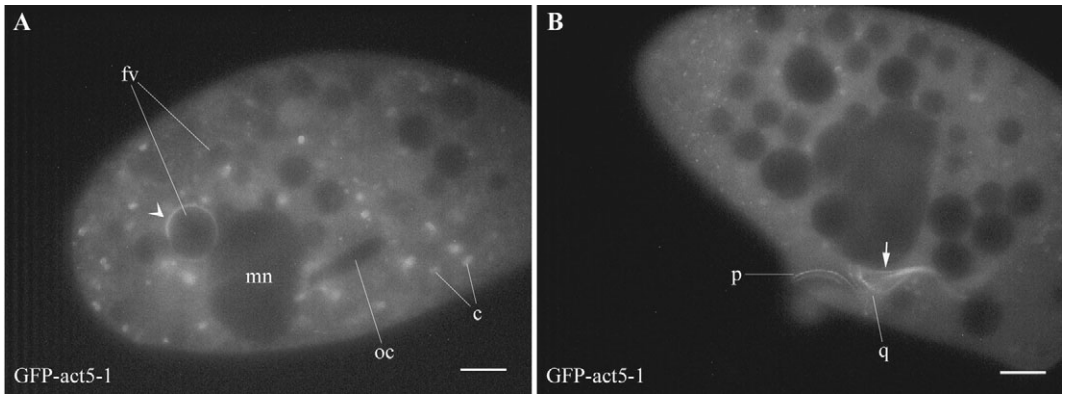

Fig. 5. GFP localization of act5-1. GFP-tagged act5-1 occurs predominantly throughout the cytoplasm, although it is also found on individual food vacuoles (fv) (arrowhead, A). The focus plane in B reveals a strong signal on different structures of the oral cavity, e.g. the peniculus (p) and the quadrulus (q). A dynamic fiber system emanating from the oral apparatus, also labeled, is indicated by an arrow. mn, macronucleus; oc, oral cavity; c, crystals. Bars, 10 μm.

Paramecium cells fed with the act9 silencing construct obtained a triangular cell shape (Fig. 8C).

Swimming behavior

The general swimming behavior of *Paramecium* cells was also analyzed. Cells silenced in act2 or act3 showed similar phenotypes. Swimming was impaired as cells were stagnant and accumulated at the bottom of the wells. Cells silenced in act4 showing the boomerang phenotype and cells silenced in act9 with a triangular shape were swimming in narrow circles, probably because of their morphological changes. Other silencing constructs had no effect on the swimming behavior. The swimming reaction upon depolarization or hyperpolarization of the plasma membrane – pronounced backward swimming in the first and accelerated forward swimming in the latter case – was not impaired in any of the silencing assays (Table 3).

Exocytosis of trichocysts

We considered that cytochalasin B treatment abolished trichocyst docking in *Paramecium* (Beisson and Rossignol, 1975) and the occurrence of anti-actin antibody labeling around trichocysts docked at the plasma membrane (Kissmehl et al., 2004). With ongoing cell divisions, every daughter cell has to produce a new arsenal of trichocysts and to transport them to the cell cortex. If any of the actin subfamilies play an essential role within this process, after 96 hours of feeding (approximately 16 fissions) a reduced number of docked trichocysts would be expected. None of the silencing constructs led to a reduction in exocytosis, except 'boomerang' cells (silenced in act4) where the exocytotic capacity was reduced to 10% (Table 3).

Phagocytosis

To analyze the formation and fission of food vacuoles and the possible role of specific actin subfamilies in the process of phagocytosis, *Paramecium* cells were fed with Congo-Red-stained yeast to visualize newly formed food vacuoles. Cells silenced in act2, act3, act4, act7 or act9 were found to have a significantly reduced number of yeast cells taken up, compared with control cells (Fig. 9). Although silencing of act7 reduced the phagocytotic capacity of the cells to ~70%, silencing of act2 or act3 reduced phagocytosis to 30%. With cells silenced in act4, phagocytosis was reduced to 30% and to 70% with cells silenced in act9, provided cells had retained normal morphology. In contrast, triangle cells (act9) had a phagocytotic capacity of only 10%, whereas in boomerang cells (act4) no new food vacuoles were generated at all (Fig. 9, Table 3).

Contractile vacuole complex and cyclosis

In cells silenced in act9 with a triangle shape, the contractile vacuole complex was severely perturbed. The filling and expelling cycle was increased from a value of 10-15 seconds in control cells to more than 100 seconds (Fig. 10). It is noteworthy that no method has demonstrated the occurrence of any actin isoform in the osmoregulatory system. Therefore, any actin silencing effects are probably due to indirect effects outside the system itself. No other subfamily silencing impaired the contractile vacuole complex (Table 3). In triangular cells, the velocity of cyclosis was accelerated two to three times when compared with control cells (Table 3) – an aspect that is difficult to explain without more detailed studies being performed.

Salient features of results

A variety of actin isoforms are expressed in *Paramecium*, frequently with a specific localization and concomitantly with a specific function. Many of the aspects we describe have remained undetected in previous affinity labeling studies with *Paramecium*. Some of our results are without precedent, also in other cells. The localization of isoforms from different families can overlap. Particularly, the interaction of actin isoforms with phagosomes is very complex. Some other isoforms have a distinct localization, e.g. in the cleavage furrow, in cilia or in some other prominent cytoskeletal aggregates. It should be stressed, however, that we do not claim that any of the prominent filamentous structures of *Paramecium* would be exclusively or predominantly made up of actin. However, intermingling with actin is a feature known from different cytoskeletal components in other cells (Manneville et al., 2003; Lin et al., 2005).

Discussion

Comparison with previous localization studies

Previously we localized actin in *Paramecium* by using fluorescently tagged DNase, heavy meromyosin, phalloidin and anti-actin antibodies (Tiggemann and Plattner, 1981; Kersken et al., 1986a; Kersken et al., 1986b) and, more specifically, using anti-actin1-1 antibodies (Kissmehl et al., 2004). Altogether this resulted in labeling of cilia, basal bodies,

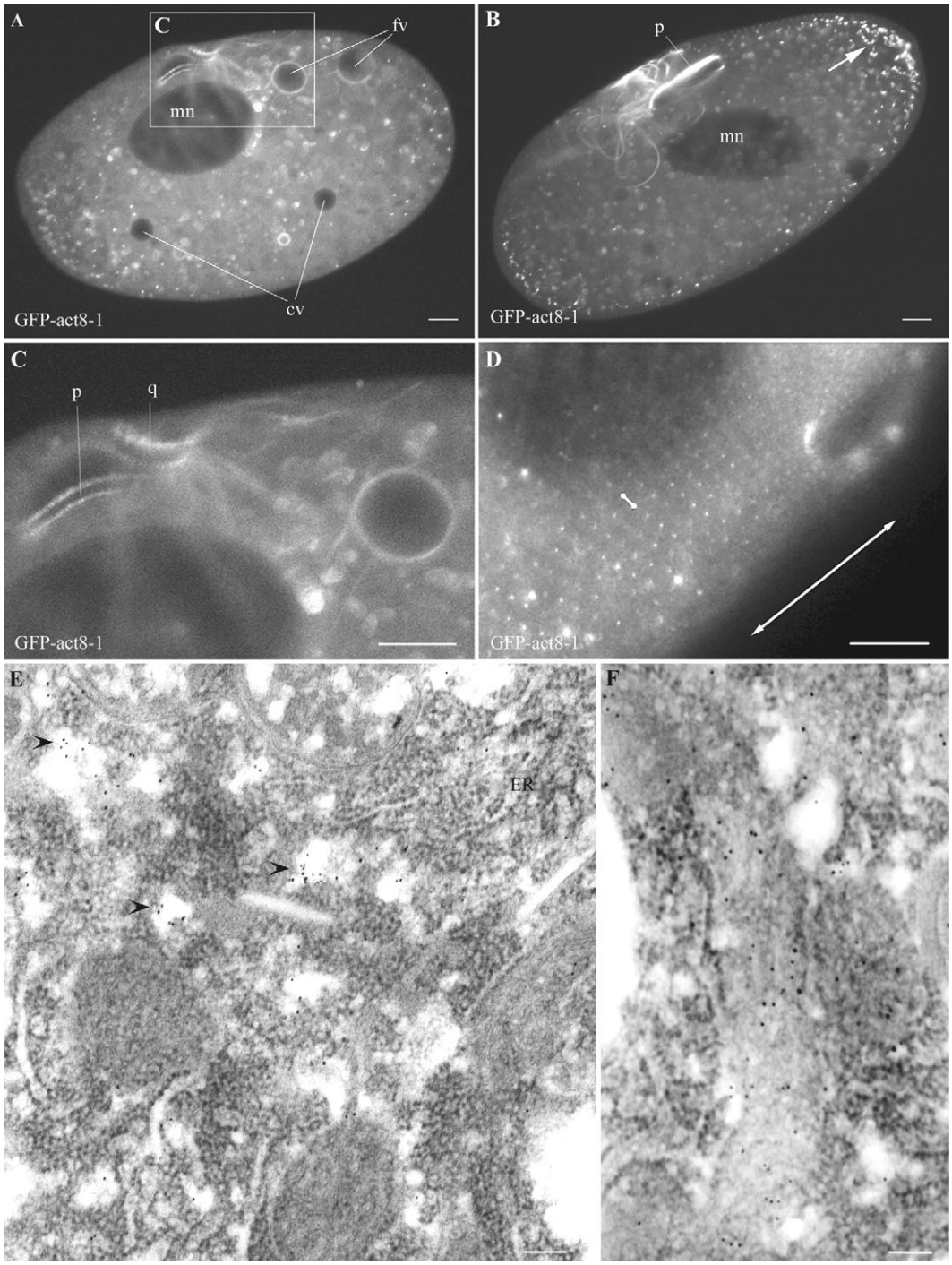

Fig. 6. Transformation of *Paramecium* cells with the GFP-act8-1 construct resulted in a weak cytosolic signal, labeling around some food vacuoles (fv; A,C) and at the presumed peniculus (p) and the quadrulus (q) of the oral cavity (A,B; C, detail from A). From the latter, a dynamic fiber system originates (B, see also supplementary material Movie 2). Close to the surface round to elongate structures are labeled (arrow in B) which continue deeper into the cytoplasm and probably represent Golgi fields (see text). The superficial plane in D reveals regularly spaced, labeled, very small dots at the plasma membrane (small bar between two labeled structures measures 2 μm; double arrow represents direction of cell axis), i.e. the sites occupied by 'parasomal sacs'. (E,F) In immunogold EM analyses, using anti-GFP gold-antibody, label was enriched at the boundary of the rough ER in association with smooth vesicular, round to elongate membrane-bounded elements (arrowhead in E) or in bona fide Golgi fields (F). mn, macronucleus; oc, oral cavity; cv, contractile vacuole. Bars, 10 μm (A-D); 100 nm (E,F).

Table 3. Effects of RNAi of specific actin subfamilies on cell shape and various behavioral and physiological aspects

Actin subfamily	Cell shape	Swimming behavior	De-/hyper-polarisation response	Exocytosis	Phagocytosis†	Contractile vacuole cycle	Cyclosis
actin1-2	Normal	Normal	Normal	100%	100%	Normal	Normal
actin1-6	Normal	Normal	Normal	100%	100%	Normal	Normal
actin1-9	Normal	Normal	Normal	100%	100%	Normal	Normal
actin2	Normal	Slower	Normal	100%	30%	Normal	Normal
actin2-1 (133bp)	Normal	Slower	Normal	100%	30%	Normal	Normal
actin2-1 (430bp)	Normal	Slower	Normal	100%	30%	Normal	Normal
actin3	Normal	Slower	Normal	100%	30%	Normal	Normal
actin3-1 (487bp)	Normal	Slower	Normal	100%	30%	Normal	Normal
actin3-1/3-2	Normal	Slower	Normal	100%	30%	Normal	Normal
actin4	Normal	Normal	Normal	100%	30%	Normal	Normal
	*boomerang**	Circles	Normal	<10%	0%	Normal	Normal
actin5	Normal	Normal	Normal	100%	100%	Normal	Normal
actin6	Normal	Normal	Normal	100%	100%	Normal	Normal
actin7	*dolphin**	Normal	Normal	100%	70%	Normal	Normal
actin8	Normal	Normal	Normal	100%	100%	Normal	Normal
actin9	Normal	Normal	Normal	100%	70%	Normal‡	Normal
	*triangle**	Circles	Normal	100%	10%	Prolonged‡	Accelerated

For the subfamilies act2 and act3, constructs of different length were designed. Within each subfamily, the different constructs showed the same effect on the cell, excluding silencing variation owing to the length of the introduced dsRNA or cross-silencing of other subfamilies. Gene silencing of members of the actin1 subfamily or act5, act6 or act8 had no effect on any of the examined aspects. For more details, see text. *See Fig. 8. †See Fig. 9. ‡See Fig. 10.

oral cavity, surface of food vacuoles, cytoproct, infraciliary lattice, cell surface ridges, the complex formed by the cortical calcium stores (alveolar sacs) and the cell membrane, surroundings of trichocyst docking sites, between bundled microtubules and ⩽1.0 μm-sized vesicles.

Although these studies anticipated part of our current results, the abundance of actin paralogs found in the context of the *Paramecium* genome project suggested a more complicated pattern. By overexpression as GFP-fusion proteins and with subfamily-specific antibodies, a variety of new and detailed features for specific isoforms emerged.

Aspects of current localization studies and their functional implications

Cytosolic compartment

The role of actin isoforms with predominantly or exclusively diffuse cytosolic localization (Table 2) is difficult to appreciate. In Apicomplexans the cause of the large percentage of G-actin is still unresolved, but physical properties unique to apicomplexan actins, as well as interaction with monomer-binding proteins, might play a role (Baum et al., 2006). Remarkably, maintenance of cytosolic actin is vital for *Drosophila* although the reasons for this remain unknown (Wagner et al., 2002).

Cilia

Occurrence of actin in cilia has been ascertained already (Tiggemann and Plattner, 1981; Kissmehl et al., 2004). We now show specifically the presence of actin2-1, actin3-1, actin4-1 and actin5-1 in cilia. Actin might serve positioning of the inner dynein arms just as in *Chlamydomonas* flagella (Hayashi et al., 2001; Yanagisawa and Kamiya, 2001).

Swimming behavior is affected by silencing genes for actin2, actin3, actin4 and actin9, all but actin9 certainly occurring in cilia (Table 3). With actin4 and actin9, this could be due to a change in cell shape. Since phagocytosis is reduced, also after silencing of these genes, reduced food supply could compromise cells in their swimming activity. However, there was no effect on the swimming behavior upon de- or hyperpolarization.

Cell cortex structures

GFP-actin3-1 outlines the ridges of the egg-box-shaped cell surface. A similar staining pattern is seen with anti-actin4-1 and anti-actin5-1 antibodies. This pattern resembles that of the outer lattice, a fibrous network sustaining the plasma membrane and delineating each cortical unit (Allen, 1971; Cohen and Beisson, 1988; Iftode et al., 1989). GFP-actin8-1 is localized, among others, to parasomal sacs (Fig. 6D), which are known to represent coated pits (Allen, 1988). Our identification relies on the small size of labeled dots and their very regular arrangement, both largely excluding any other

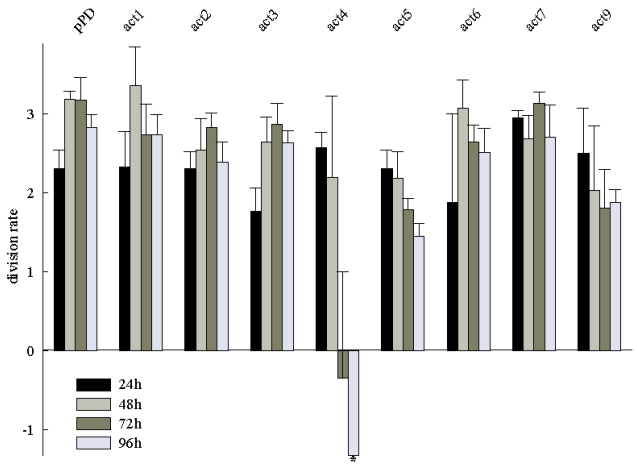

Fig. 7. Comparison of the division rate of cells silenced in different actin subfamilies. Only silencing of act4 and act9 affects the division rate, all other subfamilies show no significant difference when compared with the control (empty pPD vector). While silencing of act9 caused delayed growth, cells silenced in act4 stop dividing and start dying at 72 hours. Error bars represent s.e.m. *s.e.m.=0.

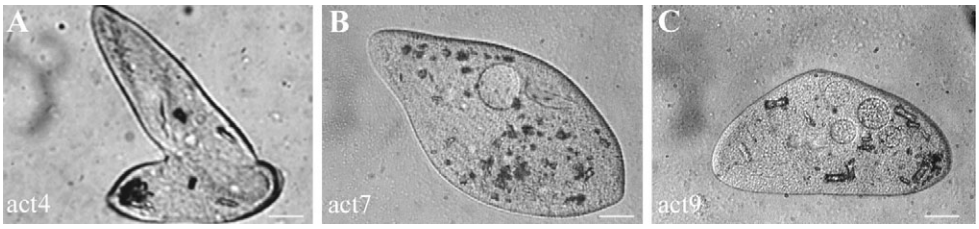

Fig. 8. Morphological changes in cells silenced in act4, act7 or act9. Cells silenced in act4 (A) are not able to divide, thus resulting in a 'boomerang' appearance. Cells silenced in act7 become slightly oversized with a pointed anterior end ('dolphin' shape, B). Silencing in act9 results in triangle-shaped cells (C). Bars, 10 μm.

surface structures. This corresponds to the complex role of actin in endosome formation at the cell membrane, as established for higher eukaryotes (Merrifield et al., 2002; Merrifield, 2004; Kirkham and Parton, 2005; Yarar et al., 2005).

Oral cavity and phagosomes

Although actin was known to occur around the oral cavity of *Paramecium* (Cohen et al., 1984; Kersken et al., 1986b) we now can specify this for actin5 and actin8. They are associated with the bona fide peniculus and quadrulus structures, as defined by Allen (Allen, 1988), but also beyond, and as part of the oral cavity lining (Kissmehl et al., 2004) and the oral filament system. In this context the mobility of these fibers must be emphasized (see supplementary material Movie 2), which could be construed as an auxiliary mechanism to guide the processing food vacuole when leaving the buccal cavity. The identification of actin8-1 as part of the endosomal system, as described above, corresponds to the labeling of the quadrulus and peniculus. These oral elements contain a large number of parasomal sacs, arranged in several rows (Allen et al., 1992).

Involvement of F-actin in phagosome formation in general (Kjeken et al., 2004) and in *Paramecium* in particular has been repeatedly documented (see above). Beyond that, several functions in the lifespan of a phagosome may require specific actins.

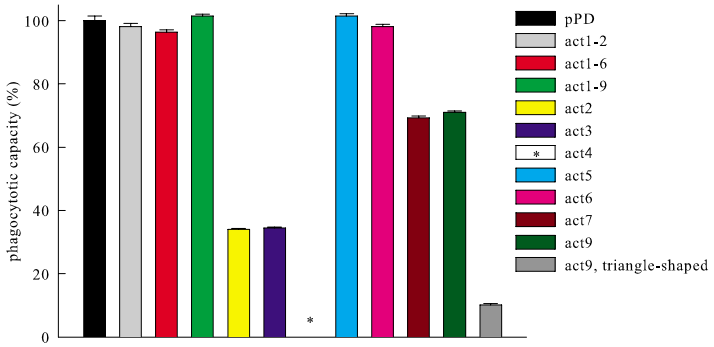

Fig. 9. Comparison of the phagocytotic capacity (as defined in Materials and Methods) of cells silenced in different actin subfamilies. Although silencing of members of the act1 subfamily, act5 or act6 does not significantly affect phagocytosis (P<0.05; control: pPD vector), it is reduced to ~70% in cells silenced in act7, and to ~30% in cells silenced in act2 or act3. With act9, in normally shaped cells phagocytosis is slightly impaired, whereas there is a strong inhibition in triangle-shaped cells (~10% phagocytotic activity). In cells silenced in act4, no phagocytosis could be observed (*). Data were collected from five different experiments from at least 20 cells per group. Error bars represent s.e.m.

The surface of some phagosomes displays a speckled appearance of GFP-actin. This can reflect a functional mosaic pattern whereby some vesicles fuse and others pinch off during circulation through the cell (Allen and Fok, 1983; Allen and Fok, 2000; Fok et al., 1985; Allen et al., 1995). For instance, vacuole fusion in yeast requires F-actin disassembly (Wang et al., 2003).

Fig. 9 shows inhibition of phagocytosis by silencing the actin genes of subfamily 2, 3, 4 or 9, particularly when the resulting cells are of aberrant morphology (Table 3). Since aberrant cells are also impaired in their swimming behavior, with the cells moving in small circles, reduced phagocytosis may be due to the effects of reduction of ciliary activity and further processing of phagosomes on engulfing bacteria. Remarkably, the actin isoforms investigated are localized to cilia by GFP or antibody labeling. However, indirect effects of an unknown kind might also play a role.

Cyclosis

Cyclosis is an established actin-dependent process (Shimmen and Yokota, 2004) also occurring with phagosomes in *Paramecium* (Sikora et al., 1979). In *Tetrahymena*, an unconventional myosin is required for directed phagosome transport (Hosein et al., 2005), but no unilateral actin arrangement has been seen. By contrast, in *Paramecium* we surprisingly see GFP-actin isoforms (actin1-2 and actin1-9), attached unilaterally to the lee side, as if pushing phagosomes. This is reminiscent of the actin-based propulsion of *Listeria* and related pathogenic bacteria (Tilney and Portnoy, 1989).

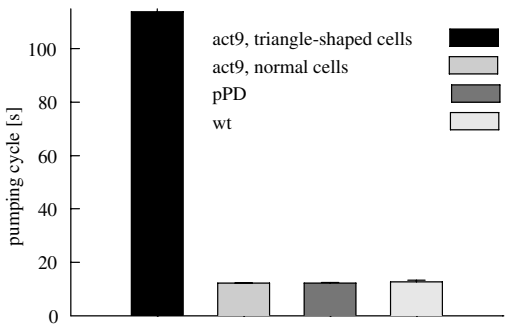

Fig. 10. Silencing of act9 affects the pumping cycle of the contractile vacuoles in misshapen transformants. While the osmoregulatory complex works normally in act9-silenced cells with normal shape, its pumping cycle is strongly prolonged in triangle-shaped cells. Feeding with pPD vector does not cause any defect in the cycle of the contractile vacuole complex. Data were collected in three different experiments from at least ten cells per group. wt, wildtype. Error bars represent s.e.m.

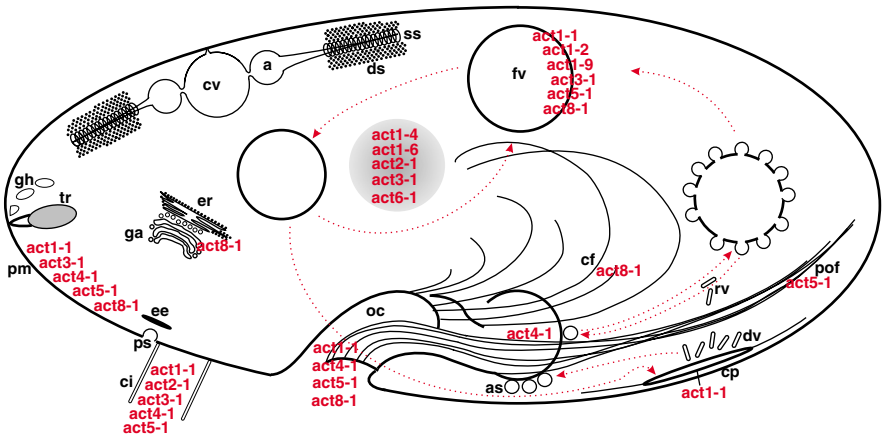

Fig. 11. Schematic distribution of actin isoforms in the *Paramecium* cell, as outlined in Table 1. The trafficking scheme is based on published reviews (Fok and Allen, 1990; Allen and Fok, 2000; Plattner and Kissmehl, 2003). Actin distribution is based mainly on the present data obtained with GFP localization in vivo and with antibody labeling, but also takes into account data from previous work (Tiggemann and Plattner, 1981; Kersken et al., 1986a; Kersken et al., 1986b; Kissmehl et al., 2004). The scheme contains elements of the osmoregulatory system (a, ampula; cv, contractile vacuole; ds, decorated spongiome; ss, smooth spongiome), though consistently unlabeled, of the phagosomal apparatus (as, acidosomes; cf, cytopharyngal fibers; cp, cytoproct; ci, cilia) dv, discoidal vesicles and other recycling vesicles, rv; ee, early endosome; er, endoplasmatic reticulum; fv, food vacuole; ga, golgi apparatus; gh, ghosts (from released trichocysts); oc, oral cavity; pm, plasma membrane; pof, post oral fibers; ps, parasomal sacs; tr, trichocysts; gray background, cytosolic.

Although the actin tails are short and not seen with immunostaining using anti-actin1-1 antibodies, their occurrence during overexpression may indicate a way of vesicle propulsion during cyclosis.

Rod-shaped organelles

GFP-actin8-1 also stains rod-shaped, ⩽1.0-μm-long organelles scattered throughout the cytoplasm, with some enrichment towards the cell surface (Fig. 5B). According to size, form and position, as well as their number these structures may correspond to the numerous Golgi elements found in *Paramecium* (Estève, 1972). In immunogold EM analysis, label was enriched at the boundary of the rough ER (Fig. 6E,F), but overexpression might have distorted Golgi stacks, as observed in *Trypanosoma* cells (García-Salcedo et al., 2004), so they could not be identified unequivocally. The labeling resembles that achieved with the GFP fusion protein of the a8 subunit of the V-ATPase in *Paramecium*, which was shown to be associated with the Golgi complex (Wassmer et al., 2006).

Nuclear and cell division

Our observation that the micronuclear cytospindle contains actin4 according to antibody labeling is compatible with a role of actin in nuclear positioning (Starr and Han, 2003). The notorious failure to demonstrate F-actin in the cleavage furrow of *Paramecium* (Kersken et al., 1986a) is apparently due to the absence of phalloidin-binding motifs in the actin4 that forms this structure (our unpublished results). Using specific antibody labeling we were successful in visualizing this structure (Fig. 4B-F). Concomitantly, silencing of the actin4 genes inhibits cell division (Fig. 7A). In *T. thermophila*, silencing of the act1 gene impairs phagocytosis, motility and cell separation (Williams et al., 2006). The failure of twisting apart was followed by a progressive re-integration of the two daughter cells. Observing numerous single cells, we could not find this phenomenon in *P. tetraurelia* silenced in actin4. We found cells arrested in early ‘post-fission’ stages, which neither grew nor divided anymore, and cells arrested during cell division. Note that the silencing effect may occur during different cell-cycle phases because *P. tetraurelia* cultures are not amenable to synchronization.

Cortical actin, cell shape and other effects

Localization of cortical F-actin and its effects can be intriguing. On the EM level, anti-actin1-1 antibodies labeled the narrow space between the plasma membrane and alveolar sacs (Kissmehl et al., 2004). In related Apicomplexans equivalent structures are also connected by short F-actin strands (Jewett and Sibley, 2003). A similar structure/function effect is discussed for mammalian cells whose cortical Ca^{2+} stores may be positioned by F-actin (Rosado and Sage, 2000; Wang et al., 2002; Roderick and Bootman, 2003; Turvey et al., 2005). Although we could not show such an effect in response to cytochalasin in *Paramecium* (Mohamed et al., 2003), this may be due to the involvement of drug-insensitive isoforms. Any disturbance, e.g. by gene silencing, may entail the considerable effects on cell form and performance, as we describe.

Some of the *Paramecium* actins may contribute to cell shaping, as seen by changes following silencing of actin7 or actin9 genes (Fig. 8B,C). Among them, only silencing of actin9 affected the division rate (Fig. 7).

In addition, silencing of actin9 considerably increased the time elapsed between expulsions of the contractile vacuole (Fig. 10). Since no actin isoform has been seen associated with the osmoregulatory system so far, the effects may be very indirect. One hypothetical possibility would be the interaction of actin with transport systems or ion channels (Fukatsu et al., 2004), which then might affect the performance of the contractile vacuole.

In the present work we show a specific localization and

functional diversification of a plethora of actin isoforms in *P. tetraurelia*. The highly regular pattern of a *Paramecium* cell, with a membrane-trafficking system with distinct, predictable pathways, provides a worthwhile and interesting system to study the mechanisms of intracellular vesicle trafficking with the involvement of a highly differentiated actin multigene family.

Materials and Methods

Stocks and cultures

Wild-type *Paramecium* cells derived from stock 51s were used, i.e. d4-2 cells for microinjection of GFP constructs and 7S cells for additional experiments. Cells were cultivated at 25°C in a decoction of dried lettuce inoculated with *Enterobacter aerogenes*, supplemented with 0.4 μg/ml β-sitosterol (Sonneborn, 1970).

Heterologous expression and purification of *Paramecium* actin-specific peptides

For heterologous expression of peptides of actin4-1 and 5-1, we selected regions of the proteins with less than 25% identity to other subfamilies to obtain subfamily-specific antibodies. Within these subfamilies, the identities at these regions were more than 90% at the amino acid level (I.M.S., J.M., C.R., E. Wagner, H.P. and R.K., unpublished), ensuring that each member of one subfamily will be recognized by the antibodies. After changing all deviant *Paramecium* glutamine codons (TAA and TAG) into universal Glutamine codons (CAA and CAG) by PCR, the coding regions of either M1-A160 (actin 4-1) or H175-L290 (actin 5-1) were cloned into the *Nco*I-*Xho*I restriction sites of pRV11a vector, which contains a His_6 tag for purification of the recombinant peptides.

Recombinant actin4-1 and actin 5-1 peptides were purified by affinity chromatography on Ni^{2+}-nitrilotriacetate agarose under denaturating conditions, as recommended by the manufacturer (Novagen, Darmstadt, Germany). The recombinant peptides were eluted with a pH gradient, pH 8 to pH 4.5, containing 8 M urea in 100 mM sodium phosphate buffer. The fractions collected were analyzed on SDS polyacrylamide gels, and those containing the recombinant peptide were pooled and dialyzed in phosphate-buffered saline (PBS).

Antibodies

Antibodies against the two recombinant actin peptides act4-1 and act5-1 were raised in rabbits. After several boosts, positive sera were taken at day 60 and affinity purified on a column loaded with the corresponding actin peptide. Finally, both sera were crosspurified against each other.

Electrophoresis and western blots

Protein samples were boiled and subjected to electrophoresis on 10% SDS polyacrylamide gels as previously described (Kissmehl et al., 2004). Gels were stained with Coomassie Blue R250 or prepared for electrophoretic protein transfer onto nitrocellulose membranes. Protein blotting was performed at 1 mA/cm^2 for 1 hour using the semidry blotter from Bio-Rad (Munich, Germany). Antibodies were diluted 1:1000 in 0.5% (w/v) non-fat dry milk and Tris-buffered saline, pH 7.5, and applied overnight at 4°C. Antibody binding was visualized by a second antibody coupled to peroxidase using an enhanced chemiluminescence detection (ECL) kit according to the manufacturer (Amersham Biosciences, Freiburg, Germany).

Immunofluorescence labeling

Cells were washed twice in 5 mM PIPES buffer, pH 7.0, containing 1 mM KCl and 1 mM $CaCl_2$, fixed in 4% (w/v) formaldehyde for 20 minutes at room temperature (RT) and then permeabilized and fixed in a mixture of 0.5% digitonin and 4% formaldehyde, dissolved in 5 mM PIPES buffer, pH 7.0, for 30 minutes. Cells were washed twice in PBS, twice for 10 minutes in PBS with 50 mM glycine added and 10 minutes in this solution with 1% bovine serum albumin (BSA) added. The rabbit anti-actin antibodies were applied at a dilution of 1:50 in PBS (+1% BSA) for 90 minutes at RT. After four 15-minute washes in PBS, FITC-conjugated anti-rabbit antibodies (Sigma-Aldrich, St Louis, MO), diluted 1:100 in PBS (+1% BSA), were applied for 90 minutes, followed by four 15-minute washes in PBS. Samples were shaken gently during all incubation and washing steps. Cells were mounted on coverslips with Mowiol supplemented with n-propylgallate to reduce fading and analyzed either in conventional Axiovert 100TV or 200M fluorescence microscopes or in a confocal laser-scanning microscope (CLSM 510) equipped with a Plan-Apochromat objective lens (all Carl Zeiss, Jena, Germany). Images acquired with the ProgRes C10plus camera and ProgRes Capture Basic software (Jenoptik, Jena, Germany) were processed with Photoshop software (Adobe Systems, San Jose, CA).

GFP constructs

For overexpression of actin, the pPXV-eGFP vector or pPXV-eGFPmcs vector (Wassmer et al., 2006) were used (eGFP, enhanced green fluorescent protein) (Hauser et al., 2000). All genes were cloned between *Spe*I and *Xho*I sites in-frame with the gene encoding GFP, except act8-1 where *Stu*I was used instead of *Spe*I because of an internal *Spe*I restriction site. PCR primers used were as follows: act1-2, 5′aA2, 5′-GCTCTAGAGAGGAACAGCATCAGCA-3′ and 3′aAX, 5′-CCGCTCGAGTCAGAAACACTTTCTGTGAACAATGG-3′; act1-4, 5′aA4 5′-GCTCTAGAGAGGAACAGCATCAGCAGGCCTATGAGTGAAGAACATCCAGC-3′ and 3′aA4X, 5′-CGGCTCGAGTCAGAAGCATTTTCTATGAACC-3′; act1-6, 5′SpeI-Act1.6, 5′-GCGACTAGTATGTAAGCTTAATATCCAGC-3′ and 3′Xho-Act1.6END, 5′-CCGCTCGAGTCAGAAACATTTTCTGTGAAC-3′; act1-9, 5′Spe-Act1-9, 5′-GGACTAGTATGAATGATGAAAAACCAGCAGTCG-3′ and 3′Xho-Act1-9, 5′-CCGCTCGAGTCAAGTGACTGTCTAACATTTTCTGTG-3′; act2-1, 5′bA1, 5′GCTCTAGAGAGGAACAGCATCAGCAGGCCTATGGACGA-CGTAATCCCAGTTG-3′ and 3′bAX, 5′-CCGCTCGAGTCAGAAGCATTTTCT-GTGCACATAACC-3′; act4-1, 5′Spe-Act4-1,5′GGACTAGTATGAATAGCGAT-GAAATAATA-3′ and 3′Xho-Act4-1, 5′CCGCTCGAGTCAATTAGGACACTTT-CTTTCTA-3′; act5-1, 5′SpeI-Act5.1, 5′GCGACTAGTATGGATAATGACATA-TTTGCTAATAACT-3′, 3′Xho-Act5.1, 5′CCGCTCGAGTCACAATTATTTTTT-GATTAAAATG-3′; act6-1, 5′SpeI-Act6.1, 5′GCGACTAGTATGGAAAGTGAG-TATGACTAAAAAG-3′, 3′Xho-Act6.1, 5′-CCGCTCGAAGTCAAAATGTTCT-CTTATGAATAAG-3′; act8-1, 5′Stu-Act8.1, 5′-GAAGGCCTATGAATAATAAT-GATTCCACCTTCTATTA-3′, 3′Xho-Act8.1, 5′-CCGCTCGAGTCAAAAGCAC-TTTCTTTATACTA-3′.

PCR reactions and cloning were carried out according to standard procedures. To avoid possible disturbance of (de-)polymerization and localization, GFP was cloned at the N-terminus of the gene of interest, separated by an 11-amino-acid spacer (Doyle and Botstein, 1996; Verkhusha et al., 1999; Wetzel et al., 2003).

Microinjection of GFP constructs

Plasmid DNA was prepared with a plasmid midi kit (Qiagen, Hilden, Germany) according to the manufacturer's protocol. 50 μg of plasmid DNA was linearized by digestion with 20 units of *Sfi*I overnight at 50°C. The DNA was precipitated with 1/10 (v/v) 3 M sodium acetate pH 5.2, with 2.5 (v/v) ethanol added, and incubated for 60 minutes at –20°C. DNA was pelleted by centrifugation, washed with 70% (v/v) ethanol and dried. The pellet was resuspended in 10 μl Millipore-filtered water and centrifuged for 30 minutes at 4°C. Microinjection of the DNA into the macronucleus was carried out as previously described (Froissard et al., 2002).

Immunoelectron microscopy

Cells derived from clones transformed with GFP-act8-1 were fixed for 1 hour on ice with 8% formaldehyde + 0.1% glutaraldehyde in PBS, pH 7.4, followed by two washes in PBS, pH 7.4 at RT. Cells were dehydrated in an ethanol series followed by embedding in LR-Gold resin (London Resin, London, GB). Ultrathin sections were decorated with affinity-purified, polyclonal anti-GFP antibody (Wassmer et al., 2006), followed by protein A-gold (5 nm) conjugates (Dept. Cell Biol., Univ. Utrecht, Utrecht, NL). These and any further steps for electron microscope immuno-analysis were essentially as described (Kissmehl et al., 2004).

Gene silencing constructs

The double T7-promotor plasmid pPD129.36 described by Fraser et al. (Fraser et al., 2000) was used. The following primers were used.

act1-2, 5′aA2Xba1, 5′-GCTCTAGAGAGGAACAGCATCAGCA-3′, 3′aAX, 5′-CCGCTCGAGTCAGAAACACTTTCTGTGAACAATGG-3′; act1-6, 5′Xba-Act1.6, 5′-GCTCTAGAAAATAGGTATAGCGGGAGATGAT-3′ and 3′Xho-Act1.6, 5′-CCGCTCGAGCAAAAACAGGTACGCAATGAG-3′; act1-9, 5′Xba-Act1-9, 5′-GCTCTAGAATGAATGATGAAAAACCAGCAGTCG-3′ and 3′Xho-Act1-9, 5′-CCGCTCGAGTCAAGTGACTGTCTAACATTTTCTGTG-3′; act2-1, 5′Xba-Act2-1, 5′-GCTCTAGAAAGTAGCCTGGTCAAATGG-3′ and 3′Xho-Act2-1, 5′-CCGCTCGAGCATATCATCCCAACGAGTG-3′; act3-1, 5′Xba-Act3-1, 5′-GCTCTAGATACAGGATTCTAAATAAAACAA-3′, 3′Spe-Act3-1, 5′-GGA-CTAGTCTATTCCATAGCCTCCC-3′, 5′Stu-Act3-1, 5′-GAAGGCCTATGATAG-AATCTCATCCTCCTGTTG-3′, 3′Xba-Act3-1, 5′GCTCTAGATCAAAAACATT-TAATGTGAGCAATC-3′; act3-2, 5′Spe-Act3-2, 5′-GGACTAGTTACAAGAAT-CTTAAACGATTAA-3′, 3′Xho-Act3-2, 5′-CCGCTCGAGCTATCTCTATAGATT-CCC-3′; act4-1, 5′Xba-Act4-1(518-535), 5′GCTCTAGAAAGCGCCAATCG-GAGGAG-3′, 3′Xho-Act4-1(885-903), 5′-CCGCTCGAGTGGTGCCAAAGCA-GACAAG-3′, act5-1, 5′Xba-Act5-1, 5′-GCTCTAGATATTGACTGAACCTCCT-TATG-3′, 3′Xho-Act5-1; 5′-CCGCTCGAGGTACCTTGCTCTTCTCAAC-3′; act6-1, 5′Xba-Act6.1, 5′-GCTCTAGACTGCTGTTTTAAATAAGTCTG-3′ and 3′Xho-Act6.1, 5′-CCGCTCGAGTCAAAATGTTCTCTTATGAATAAG-3′; act7-1, 5′Xba-Act7-1, 5′-GCTCTAGAGGCTTACGAATTACCAGAC-3′ and 3′Xho-Act7-1, 5′-CCGCTCGAGAGCTCCCAACCAAGATGC-3′; act8-1, 5′Xba-Act8-1, 5′-GCTCTAGATTTCCAGTGGAAAAACAACAG-3′ and 3′Xho-Act8-1, 5′-CCGC-TCGAGACCATCGGGCAAATCATACA-3′; act9-1, 5′Xba-Act9-1, 5′-GCTCTA-GATTGGCAATGTACTTCCTC-3′ and 3′Xho-Act9-1, 5′-CCGCTCGAGTTC-CAAAATATGTGTCAGTG-3′. PCR reactions and cloning were carried out according to standard procedures.

Gene silencing by feeding

The RNaseIII-deficient *E. coli* strain HT115 (Timmons et al., 2001) was

transformed with the gene-silencing plasmids. Overnight cultures in Luria-Broth (LB) medium supplemented with ampicillin (amp) and tetracycline were diluted with LB/amp medium 1:100 and the new cultures were grown to an OD_{600nm} between 0.2 and 0.4. The cultures were induced with 125 μg/ml isopropyl-thio-β-D-galactopyranoside (IPTG) for 3 hours, centrifuged and the pelleted bacteria resuspended in *Paramecium* culture medium. The OD_{600nm} was adjusted with medium to 0.25 and supplemented with 100 μg/ml ampicillin and 12 μg/ml IPTG.

Single *Paramecium* cells were isolated and grown for about twenty fissions, again isolated and grown for another twenty fissions before each clone was starved to induce autogamy (Berger, 1986). Autogamy was monitored by fluorescence microscopy after staining with Hoechst 33342 (Molecular Probes, Leiden, The Netherlands). Autogamous cells were fed, first with normal bacteria and used 3 days later for RNAi feeding experiments. *Paramecium* cells were washed twice in PIPES buffer and starved for at least 2 hours in PIPES at room temperature before use in feeding experiments. In single-cell experiments, one cell was added to 150 μl feeding solution in a depression well. Cells were cultured at 25°C during the experiment and transferred every 24 hours to a freshly prepared feeding solution. The phenotype was analyzed 96 hours after the start of the feeding experiment.

Behavioral and functional assays

Cells were observed in their wells under a binocular microscope to ascertain their normal swimming behavior. For further tests, cells were transferred in 10 μl drops and observed for 30 seconds after addition of an equal volume of a twofold concentrated test solution. Depolarization of the plasma membrane, indicated by ciliary reversal and pronounced backward swimming, was induced by adding 40 mM KCl. Cells that showed any significant backward swimming events were scored as positive responders. Hyperpolarization was induced by adding 20 mM $CaCl_2$, and cells that showed accelerated forward swimming were scored as positive responders. To analyze exocytotic capacity, cells were triggered with 0.2% aminoethyldextran (Plattner et al., 1984) in a buffer consisting of 10 mM Tris-HCl, 0.1 mM $CaCl_2$, pH 7.0. Exocytotic tests were repeated with saturated picric acid, the traditional (lethal) test used in genetic studies. The division rate was calculated according to the equation:

$$n = [\log(N_2) - \log(N_1)] / \log(2) ,$$

where n is the number of divisions, N_2 is the starting number and N_1 is the end number of cells.

For evaluation of the phagocytotic capacity, cells were fed with Congo-Red-stained yeast, fixed with 4% (w/v) formaldehyde after 3, 5 and 10 minutes, and the number of yeast cells ingested was counted. The amount of yeast in control cells was set as 100% phagocytotic activity. This was evaluated in at least 20 cells per experiment, with five experiments per actin type. The decrease in phagocytotic capacity concerned the number of food vacuoles formed as well as the number of yeast cells per vacuole. Although a variation of up to 30 yeast cells per vacuole was observed in control cells, phagocytotically restricted *Paramecium* cells formed only small vacuoles with less than 10 yeast cells.

Statistical evaluation

For statistical evaluation of changes in the division rate and in the phagocytotic capacity in RNAi experiments, one-way analysis of variance (ANOVA) was used to determine statistical significance.

We gratefully acknowledge the availability of genomic library from J. Cohen (CNRS Gif-sur-Yvette, France) and of an expression library from J. E. Schultz (University of Tübingen, Germany) as well as the access to the *Paramecium* genome database at an early stage of its development (J. Cohen and L. Sperling, CNRS, Gif-sur-Yvette, as well as Genoscope, Paris). We thank C. Stuermer and E. May for use of their confocal microscopes. Supported by Deutsche Forschungsgemeinschaft grants to H.P.

References

Allen, R. D. (1971). Fine structure of membranous and microfibrillar systems in the cortex of *Paramecium caudatum*. *J. Cell Biol.* **49**, 1-20.

Allen, R. D. (1988). Cytology. In *Paramecium* (ed. H.-D. Görtz), pp. 4-40. Berlin: Springer-Verlag.

Allen, R. D. and Fok, A. K. (1983). Phagosome fusion vesicles of *Paramecium*. I. Thin-section morphology. *Eur. J. Cell Biol.* **29**, 150-158.

Allen, R. D. and Fok, A. K. (1985). Modulation of the digestive lysosomal system in *Paramecium caudatum*. III. Morphological effects of cytochalasin B. *Eur. J. Cell Biol.* **37**, 35-43.

Allen, R. D. and Fok, A. K. (2000). Membrane trafficking and processing in *Paramecium*. *Int. Rev. Cytol.* **198**, 277-317.

Allen, R. D., Schroeder, C. C. and Fok, A. K. (1992). Endosomal system of *Paramecium:* coated pits to early endosomes. *J. Cell Sci.* **101**, 449-461.

Allen, R. D., Bala, N. P., Ali, R. F., Nishida, D. M., Aihara, M. S., Ishida, M. and Fok, A. K. (1995). Rapid bulk replacement of acceptor membrane by donor membrane during phagosome to phagoacidosome transformation in *Paramecium*. *J. Cell Sci.* **108**, 1263-1274.

Aury, J.-M., Jaillon, O., Duret, L., Noel, B., Jubin, C., Porcel, B. M., Ségurens, B., Daubin, V., Anthouard, V., Aiach, N. et al. (2006). Global trends of whole-genome duplications revealed by the ciliate *Paramecium tetraurelia*. *Nature* **444**, 171-178.

Baum, J., Papenfuss, A. T., Baum, B., Speed, T. P. and Cowman, A. F. (2006). Regulation of apicomplexan actin-based motility. *Nat. Rev. Microbiol.* **4**, 621-628.

Beisson, J. and Rossignol, M. (1975). Movements and positioning of organelles in *Paramecium aurelia*. In *Nucleocytoplasmic Relationships During Cell Morphogenesis In Some Unicellular Organisms* (ed. S. Puiseux-Dao), pp. 291-294. Amsterdam, New York, London: Elsevier.

Berger, J. D. (1986). Autogamy in *Paramecium*: cell cycle stage-specific commitment to meiosis. *Exp. Cell Res.* **166**, 475-485.

Cao, H., Weller, S., Orth, J. D., Chen, J., Huang, B., Chen, J.-L., Stamnes, M. and McNiven, M. A. (2005). Actin and Arf1-dependent recruitment of a cortactin-dynamin complex to the Golgi regulates post-Golgi transport. *Nat. Cell Biol.* **7**, 483-492.

Carreno, S., Engqvist-Goldstein, A. E., Zhang, C. X., McDonald, K. L. and Drubin, D. G. (2004). Actin dynamics coupled to clathrin-coated vesicle formation at the trans-Golgi network. *J. Cell Biol.* **165**, 781-788.

Cohen, J. and Beisson, J. (1988). The cytoskeleton. In *Paramecium* (ed. H.-D. Görtz), pp. 363-392. Berlin, Heidelberg, New York: Springer-Verlag.

Cohen, J., Garreau De Loubresse, N. and Beisson, J. (1984). Actin microfilaments in *Paramecium*: localization and role in intracellular movements. *Cell Motil.* **4**, 443-468.

Damiani, M. T. and Colombo, M. I. (2003). Microfilaments and microtubules regulate recycling from phagosomes. *Exp. Cell Res.* **289**, 152-161.

Dobrowolski, J. M., Niesman, I. R. and Sibley, L. D. (1997). Actin in the parasite *Toxoplasma gondii* is encoded by a single copy gene, ACT1 and exists primarily in a globular form. *Cell Motil. Cytoskeleton* **37**, 253-262.

Doyle, T. and Botstein, D. (1996). Movement of yeast cortical actin cytoskeleton visualized in vivo. *Proc. Natl. Acad. Sci. USA* **93**, 3886-3891.

Drengk, A., Fritsch, J., Schmauch, C., Rühling, H. and Maniak, M. (2003). A coat of filamentous actin prevents clustering of late-endosomal vacuoles in vivo. *Curr. Biol.* **13**, 1814-1819.

Estève, J. C. (1972). L'appareil de Golgi des ciliés. Ultrastructure, particulièrement chez *Paramecium*. *J. Protozool.* **19**, 609-618.

Fok, A. K. and Allen, R. D. (1988). The lysosome system. In *Paramecium* (ed. H.-D. Görtz), pp. 301-324. Berlin, Heidelberg, New York: Springer-Verlag.

Fok, A. K. and Allen, R. D. (1990). The phagosome-lysosome membrane system and its regulation in *Paramecium*. *Int. Rev. Cytol.* **123**, 61-94.

Fok, A. K., Leung, S. S. K., Chun, D. P. and Allen, R. D. (1985). Modulation of the digestive lysososmal system in *Paramecium caudatum*. II. Physiological effects of cytochalasin B, colchicine and trifluoperazine. *Eur. J. Cell Biol.* **37**, 27-34.

Fraser, A. G., Kamath, R. S., Zipperlen, P., Martinez-Campos, M., Sohrmann, M. and Ahringer, J. (2000). Functional genomic analysis of *C. elegans* chromosome I by systematic RNA interference. *Nature* **408**, 325-330.

Froissard, M., Kissmehl, R., Dedieu, J. C., Gulik-Krzywicki, T., Plattner, H. and Cohen, J. (2002). N-ethylmaleimide-sensitive factor is required to organize functional exocytotic microdomains in *Paramecium*. *Genetics* **161**, 643-650.

Fukatsu, K., Bannai, H., Zhang, S., Nakamura, H., Inoue, T. and Mikoshiba, K. (2004). Lateral diffusion of inositol 1,4,5-trisphosphate receptor type 1 is regulated by actin filaments and 4.1N in neuronal dendrites. *J. Biol. Chem.* **279**, 48976-48982.

García-Salcedo, J. A., Pérez-Morga, D., Gijón, P., Dilbeck, V., Pays, E. and Nolan, D. P. (2004). A differential role for actin during the life cycle of *Trypanosoma brucei*. *EMBO J.* **23**, 780-789.

Gasman, S., Chasserot-Golaz, S., Malacombe, M., Way, M. and Bader, M.-F. (2004). Regulated exocytosis in neuroendocrine cells: a role for subplasmalemmal Cdc42/N-WASP-induced actin filaments. *Mol. Biol. Cell* **15**, 520-531.

Goodson, H. V. and Hawse, W. F. (2002). Molecular evolution of the actin family. *J. Cell Sci.* **115**, 2619-2622.

Gordon, J. L. and Sibley, L. D. (2005). Comparative genome analysis reveals a conserved family of actin-like proteins in apicomplexan parasites. *BMC Genomics* **6**, 179.

Hauser, K., Haynes, W. J., Kung, C., Plattner, H. and Kissmehl, R. (2000). Expression of the green fluorescent protein in *Paramecium tetraurelia*. *Eur. J. Cell Biol.* **79**, 144-149.

Hayashi, M., Hirono, M. and Kamiya, R. (2001). Recovery of flagellar dynein function in a *Chlamydomonas* actin/dynein-deficient mutant upon introduction of muscle actin by electroporation. *Cell Motil. Cytoskeleton* **49**, 146-153.

Haynes, W. J., Ling, K. Y., Saimi, Y. and Kung, C. (1995). Induction of antibiotic resistance in *Paramecium tetraurelia* by the bacterial gene APH-3'-II. *J. Eukaryot. Microbiol.* **42**, 83-91.

Hölttä-Vuori, M., Alpy, F., Tanhuanpää, K., Jokitalo, E., Mutka, A.-L. and Ikonen, E. (2005). MLN64 is involved in actin-mediated dynamics of late endocytic organelles. *Mol. Biol. Cell* **16**, 3873-3886.

Hosein, R. E., Williams, S. A., Haye, K. and Gavin, R. H. (2003). Expression of GFP-actin leads to failure of nuclear elongation and cytokinesis in *Tetrahymena thermophila*. *J. Eukaryot. Microbiol.* **50**, 403-408.

Hosein, R. E., Williams, S. A. and Gavin, R. H. (2005). Directed motility of phagosomes in *Tetrahymena thermophila* requires actin and myo 1p, a novel unconventional myosin. *Cell Motil. Cytoskeleton* **61**, 49-60.

Iftode, F., Cohen, J., Ruiz, F., Torres Rueda, A., Chen-Shan, L., Adoutte, A. and Beisson, J. (1989). Development of surface pattern during division in *Paramecium*. I.

Mapping of duplication and reorganization of cortical cytoskeletal structures in the wild type. *Development* **105**, 191-211.
Jewett, T. J. and Sibley, L. D. (2003). Aldolase forms a bridge between cell surface adhesins and the actin cytoskeleton in Apicomplexan parasites. *Mol. Cell* **11**, 885-894.
Kaksonen, M., Toret, C. P. and Drubin, D. G. (2006). Harnessing actin dynamics for clathrin-mediated endocytosis. *Nat. Rev. Mol. Cell Biol.* **7**, 404-414.
Kandasamy, M. K., Deal, R. B., McKinney, E. C. and Meagher, R. B. (2004). Plant actin-related proteins. *Trends Plant Sci.* **9**, 196-202.
Kersken, H., Momayezi, M., Braun, C. and Plattner, H. (1986a). Filamentous actin in *Paramecium* cells: functional and ultrastructural changes correlated with phalloidin affinity labeling in vivo. *J. Histochem. Cytochem.* **34**, 455-465.
Kersken, H., Vilmart-Seuwen, J., Momayezi, M. and Plattner, H. (1986b). Filamentous actin in *Paramecium* cells: mapping by phalloidin affinity labeling in vivo and in vitro. *J. Histochem. Cytochem.* **34**, 443-454.
Kirkham, M. and Parton, R. G. (2005). Clathrin-independent endocytosis: new insights into caveolae and non-caveolar lipid raft carriers. *Biochim. Biophys. Acta* **1745**, 273-286.
Kissmehl, R., Sehring, I. M., Wagner, E. and Plattner, H. (2004). Immuno-localization of actin in *Paramecium* cells. *J. Histochem. Cytochem.* **52**, 1543-1559.
Kjeken, R., Egeberg, M., Habermann, A., Kuehnel, M., Peryon, P., Floetenmeyer, M., Walther, P., Jahraus, A., Defacque, H. et al. (2004). Fusion between phagosomes, early and late endosomes: a role for actin in fusion between late, but not early endocytic organelles. *Mol. Biol. Cell* **15**, 345-358.
Lin, C.-M., Chen, H.-J., Leung, C. L., Parry, D. A. D. and Liem, R. K. H. (2005). Microtubule actin crosslinking factor 1b: a novel plakin that localizes to the Golgi complex. *J. Cell Sci.* **118**, 3727-3738.
Manneville, J. B., Etienne-Manneville, S., Skehel, P., Carter, T., Ogden, D. and Ferenczi, M. (2003). Interaction of the actin cytoskeleton with microtubules regulates secretory organelle movement near the plasma membrane in human endothelial cells. *J. Cell Sci.* **116**, 3927-3938.
Merrifield, C. J. (2004). Seeing is believing: imaging actin dynamics at single sites of endocytosis. *Trends Cell Biol.* **14**, 352-358.
Merrifield, C. J., Feldman, M. E., Wan, L. and Almers, W. (2002). Imaging actin and dynamin recruitment during invagination of single clathrin-coated pits. *Nat. Cell Biol.* **4**, 691-698.
Mohamed, I., Husser, M., Sehring, I., Hentschel, J., Hentschel, C. and Plattner, H. (2003). Refilling of cortical calcium stores in *Paramecium* cells: in situ analysis in correlation with store-operated calcium influx. *Cell Calcium* **34**, 87-96.
Muller, J., Oma, Y., Vallar, L., Friederich, E., Poch, O. and Winsor, B. (2005). Sequence and comparative genomic analysis of actin-related proteins. *Mol. Biol. Cell* **16**, 5736-5748.
Otegui, M. S., Verbrugghe, K. J. and Skop, A. R. (2005). Midbodies and phragmoplasts: analogous structures involved in cytokinesis. *Trends Cell Biol.* **15**, 404-413.
Plattner, H. and Kissmehl, R. (2003). Molecular aspects of membrane trafficking in *Paramecium*. *Int. Rev. Cytol.* **232**, 185-216.
Plattner, H., Matt, H., Kersken, H., Haacke, B. and Stürzl, R. (1984). Synchronous exocytosis in *Paramecium* cells. I. A novel approach. *Exp. Cell Res.* **151**, 6-13.
Pollard, T. D. (2001). Genomics, the cytoskeleton and motility. *Nature* **409**, 842-843.
Pollard, T. D., Blanchoin, L. and Mullins, R. D. (2000). Molecular mechanisms controlling actin filament dynamics in nonmuscle cells. *Annu. Rev. Biophys. Biomol. Struct.* **29**, 545-576.
Poupel, O., Boleti, H., Axisa, S., Couture-Tosi, E. and Thardieux, I. (2000). Toxofilin, a novel actin-binding protein from *Toxoplasma gondii*, sequesters actin monomers and caps actin filaments. *Mol. Biol. Cell* **11**, 355-368.
Roderick, H. L. and Bootman, M. D. (2003). Calcium influx: is Homer the missing link? *Curr. Biol.* **13**, R976-R978.
Rosado, J. A. and Sage, S. O. (2000). The actin cytoskeleton in store-mediated calcium entry. *J. Physiol.* **526**, 221-229.
Ruiz, F., Vayssié, L., Klotz, C., Sperling, L. and Madeddu, L. (1998). Homology-dependent gene silencing in *Paramecium*. *Mol. Biol. Cell* **9**, 931-943.
Sahoo, N., Beatty, W., Heuser, J., Sept, D. and Sibley, L. D. (2006). Unusual kinetic and structural properties control rapid assembly and turnover of actin in the parasite *Toxoplasma gondii*. *Mol. Biol. Cell* **17**, 895-906.
Schmitz, S., Grainger, M., Howell, S., Calder, L. J., Gaeb, M., Pinder, J. C., Holder, A. A. and Veigel, C. (2005). Malaria parasite actin filaments are very short. *J. Mol. Biol.* **349**, 113-125.
Shimmen, T. and Yokota, E. (2004). Cytoplasmic streaming in plants. *Curr. Opin. Cell Biol.* **16**, 68-72.
Sikora, J., Wasik, A. and Baranowski, Z. (1979). The estimation of velocity distribution profile of *Paramecium* cytoplasmic streaming. *Eur. J. Cell Biol.* **19**, 184-188.
Skouri, F. and Cohen, J. (1997). Genetic approach to regulated exocytosis using functional complementation in *Paramecium*: identification of the ND7 gene required for membrane fusion. *Mol. Biol. Cell* **8**, 1063-1071.
Sonneborn, T. M. (1970). Methods in *Paramecium* research. *Methods Cell Physiol.* **4**, 242-335.
Starr, D. A. and Han, M. (2003). ANCors away: an actin based mechanism of nuclear positioning. *J. Cell Sci.* **116**, 211-216.
Stoorvogel, W., Kerstens, S., Fritzsche, I., den Hartigh, J. C., Oud, R., van der Heyden, M. A. G., Voortman, J. and van Bergen en Henegouwen, P. M. P. (2004). Sorting of ligand-activated epidermal growth factor receptor to lysosomes requires its actin-binding domain. *J. Biol. Chem.* **279**, 11562-11569.
Tiggemann, R. and Plattner, H. (1981). Localization of actin in the cortex of *Paramecium tetraurelia* cells by immuno- and affinity-fluorescence microscopy. *Eur. J. Cell Biol.* **24**, 184-190.
Tilney, L. G. and Portnoy, D. A. (1989). Actin filaments and the growth, movement, and spread of the intracellular bacterial parasite, *Listeria monocytognes*. *J. Cell Biol.* **109**, 1597-1608.
Timmons, L., Court, D. L. and Fire, A. (2001). Ingestion of bacterially expressed dsRNAs can produce specific and potent genetic interference in *Caenorhabditis elegans*. *Gene* **263**, 103-112.
Turvey, M. R., Fogarty, K. E. and Thorn, P. (2005). Inositol (1,4,5)-trisphosphate receptor links to filamentous actin are important for generating local Ca^{2+} signals in pancreatic acinar cells. *J. Cell Sci.* **118**, 971-980.
Verkhusha, V. V., Tsukita, S. and Oda, S. (1999). Actin dynamics in lamellipodia of migrating border cells in the *Drosophila* ovary revealed by a GFP-actin fusion protein. *FEBS Lett.* **445**, 395-401.
Visegrády, B., Lörinczy, D., Hild, G., Somogyi, B. and Nyitrai, M. (2004). The effect of phalloidin and jasplakinolide on the flexibility and thermal stability of actin filaments. *FEBS Lett*. **565**, 163-166.
Wagner, C. R., Mahowald, A. P. and Miller, K. G. (2002). One of the two cytoplasmic actin isoforms in *Drosophila* is essential. *Proc. Natl. Acad. Sci. USA* **99**, 8037-8042.
Wang, L., Merz, A. J., Collins, K. M. and Wickner, W. (2003). Hierarchy of protein assembly at the vertex ring domain for yeast vacuole docking and fusion. *J. Cell Biol.* **160**, 365-374.
Wang, Y. J., Gregory, R. B. and Barritt, G. J. (2002). Maintenance of the filamentous actin cytoskeleton is necessary for the activation of store-operated Ca^{2+} channels, but not other types of plasma-membrane Ca^{2+} channels, in rat hepatocytes. *Biochem. J.* **363**, 117-126.
Wassmer, T., Kissmehl, R., Cohen, J. and Plattner, H. (2006). Seventeen a-subunit isoforms of *Paramecium* V-ATPase provide high specialization in localization and function. *Mol. Biol. Cell* **17**, 917-930.
Wetzel, D. M., Hakansson, S., Hu, K., Roos, D. and Sibley, L. D. (2003). Actin filament polymerization regulates gliding motility by apicomplexan parasites. *Mol. Biol. Cell* **14**, 396-406.
Wieland, T. and Faulstich, H. (1978). Amatoxins, phallotoxins, phallolysin, and antamanide: the biologically active components of poisonous *Amanita* mushrooms. *CRC Crit. Rev. Biochem.* **5**, 185-260.
Williams, N. E., Tsao, C.-C., Bowen, J., Hehman, G. L., Williams, R. J. and Frankel, J. (2006). The Actin Gene *ACT1* Is Required for Phagocytosis, Motility, and Cell Separation of *Tetrahymena thermophila*. *Eukaryotic Cell* **5**, 555-567.
Yam, P. T. and Theriot, J. A. (2004). Repeated cycles of rapid actin assembly and disassembly on epithelial cell phagosomes. *Mol. Biol. Cell* **15**, 5647-5658.
Yanagisawa, H.-A. and Kamiya, R. (2001). Association between actin and light chains in *Chamydomonas* flagellar inner-arm dyneins. *Biochem. Biophys. Res. Commun.* **288**, 443-447.
Yarar, D., Waterman-Storer, C. M. and Schmid, S. L. (2005). A dynamic actin cytoskeleton functions at multiple stages of clathrin-mediated endocytosis. *Mol. Biol. Cell* **16**, 964-975.